Conduction-Radiation Property of Ceramic and Graphite Fiber Thermal Insulation Mat

by

Hiesun SANG*, Atsumasa YOSHIDA* and Takeshi KUNITOMO*

(Received June 30, 1988)

Abstract

The thermal conductivities for four typical kinds of heat resisting fibrous thermal insulation mats were obtained by the steady state parallel plates method in a vacuum condition. These experimental results were correlated by a combined conduction and radiation heat transfer model to determine the conduction thermal conductivity and the extinction coefficient which govern the heat transfer in the layer of fibrous insulating material. On the basis of these values, a new simple method was proposed to estimate the thermal conductivities of the four materials as a function of the bulk density and the mean temperature in the insulation layer.

1. Introduction

Fibrous material is an important insulating material with many applications. It is the main source of insulation for homes in many countries, and is used extensively in aircrafts, industrial structures and so on. It is also useful for a good usage of energy by making thermal loss decrease and thermal efficiency increase.

A number of studies has been done on the heat transfer properties of fiber insulation mats[1),2),3)]. Caps et al.[4)] measured the thermal conductivities and determined the conductive and the radiative parameters on some materials. In spite of the above studies, the number of insulating materials, of which the observed thermal data have been reported, is very limited, and the prediction of the thermal conductivity at high temperatures is generally impossible.

In the present work, the thermal conductivities of four kinds of fibrous thermal insulating materials, involving three kinds of heat resisting ceramics and a kind of graphite, were measured in a vacuum condition by the steady state parallel plates method. This was done by changing the bulk density, the average

* Department of Engineering Science, Faculty of Engineering, Kyoto University, Kyoto 606, Japan

temperature and the temperature difference. Further, the extinction coefficients were obtained so as to propose a simple estimation procedure of the thermal conductivity of the four insulating materials measured here.

2. Experimental apparatus and procedure

A schematic diagram of the experimental apparatus is shown in Fig. 1. It is composed of four heaters; main heater ① of measuring part, low temperature heater ③ of heat sink, guard heater ② and auxiliary heater ④ to maintain one dimensional heat transfer through the specimen ⑥. The size of the specimen is $300 \times 300 \times 30\,t$ mm, and the measuring part is $150 \times 150 \times 30\,t$ mm. The temperatures of the heaters were controlled independently. The heater surface was coated with a heat resisting black paint whose emissivity was larger than 0.95 in the infrared region. The thickness of the specimen was determined by the spacer. The height and diameter of the vacuum chamber ⑩ are 900 mm and 700 mm, respectively. The pressure of the vacuum chamber was kept at 0.5 Pa by a vacuum pump ⑨. The temperatures were measured by chromel-alumel thermocouples of 0.1 mm diameter. The surface temperatures of the heater were controlled with the accuracy of $\pm$ 0.2 K. After keeping the steady state for about 6 hours, the heat input and the temperatures were measured.

The thermal conductivity k can be given by the following equation, when

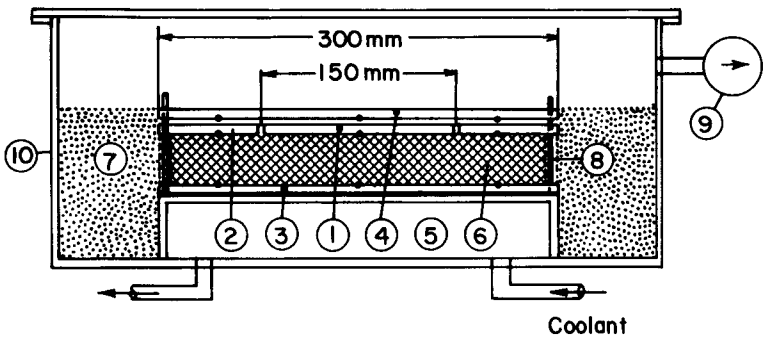

① Main Heater ② Guard Heater
③ Low. Temp. Heater ④ Auxiliary Heater
⑤ Heat Sink ⑥ Specimen
⑦ Insulation ⑧ Support Bar
⑨ Vacuum Pump ⑩ Vacuum Chamber

Fig. 1 Schematic diagram of experimental apparatus

Table 1 Chemical compositions and physical properties of specimens

	Composition (wt %)	Fiber diameter d (μm) True density of fiber ρ_o (kg/m^3)	Orientation of fiber
Specimen 1	Al_2O_3 ; 51.8 SiO_2 ; 47.9 Na_2O ; 0.2 Fe_2O_3 ; 0.1	d ; 2.6-3.0 ρ_o ; 2730	Pile of lightly woven mat; stratified
Specimen 2	Al_2O_3 ; 80 SiO_2 ; 20	d ; 3.0 ρ_o ; 3300	〃
Specimen 3	SiO_2 ; 100	d ; 6-12 ρ_o ; 2200	Randomly orientated; not woven bed
Specimen 4	Graphite; 100	d ; 12.5-15.5 ρ_o ; 1570	

ΔT is relatively small;

$$k = WL/(A\Delta T) \tag{1}$$

where W is the total heat flux, L is the thickness of the specimen, $\Delta T = (T_1 - T_2)$ is the temperature difference and A is the area of the measuring part. The experimental errors on k on the measurement of heat flux through the specimen were smaller than 5%. Four kinds of heat resisting fibrous thermal insulating materials served as the specimen. They are Al_2O_3–SiO_2 compound (Specimen 1, 50-50%, Specimen 2, 80-20%), SiO_2 100% (Specimen 3) and graphite (Specimen 4). Their chemical compositions, physical properties and the fiber structures are indicated in Table 1.

3. Results

3. 1 Experimental results

In Fig. 2, the characteristic thermal conductivities k_s of the fiber of specimen cited from the data book[5] are shown. The k_s of the specimen 4 is over 10 times larger than the others. The k_s of the specimen 3 is much smaller than the other specimens.

In the experiment, the average temperature in the specimen changed in the region from 373 K to 773 K. As for the bulk density ρ, three values of 50, 129, 183 kg/m^3 were adopted.

In Fig. 3, the relation between the observed k and ρ is shown with T_m and

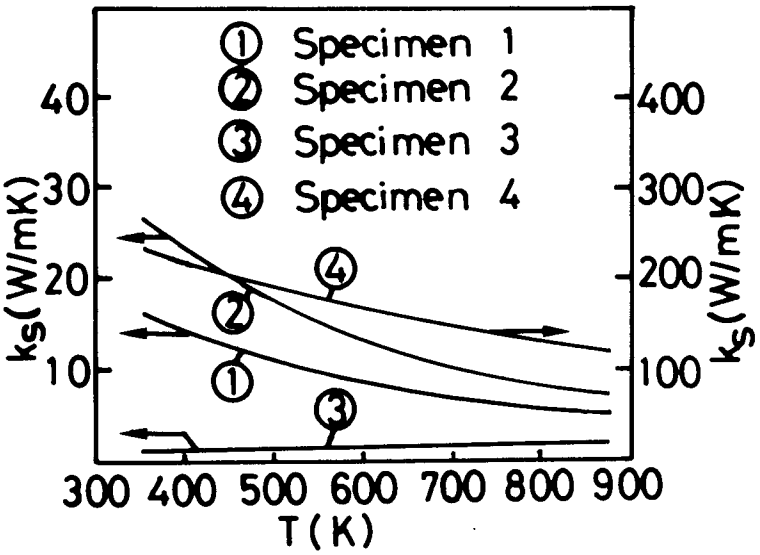

Fig. 2 Characteristic thermal conductivity of fiber

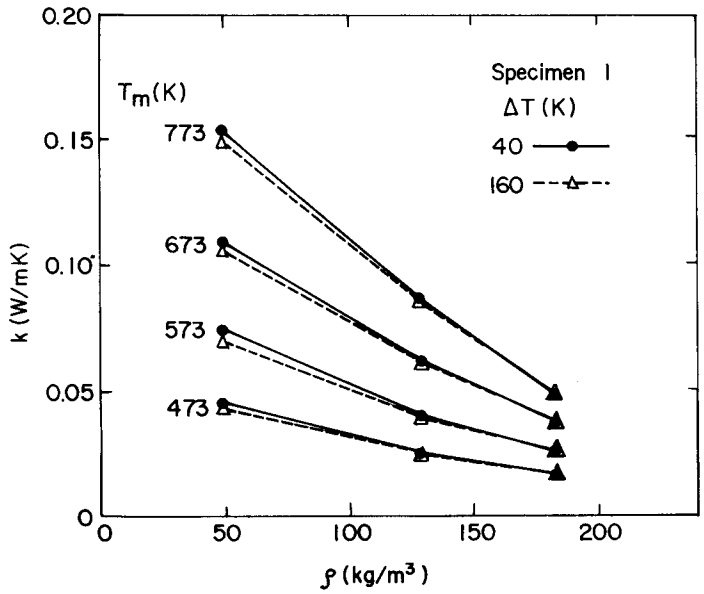

Fig. 3 Thermal conductivity vs. bulk density

ΔT as parameters for Specimen 1. The k greatly decreases with the increase of the bulk density in a range of high temperature, but less in a range of low temperature. On the other hand, k increases as T_m increases, much more in low bulk density than in high bulk density. Though the influence of the temperature

difference ΔT on k becomes slightly larger as the bulk density decreases, practically speaking, this influence is quite small in the range of the present experimental conditions. Therefore, "the averaged material temperature" T_m is allowed to be considered as "the material temperature" itself. The present observed conductivity can be considered as the physical property depending on the bulk density and the material temperature. The situations mentioned above are essentially the same for the other three specimens.

Figure 4 shows the relation between k and T_m for Specimens 1 and 4 at the three bulk densities. As seen in the figure, Specimen 1 shows a much larger temperature dependence than Specimen 4. The others, which are ceramic materials, show a similar trend to Specimen 1.

3. 2 Combined heat transfer model

In Fig. 5, the combined heat transfer model for fibrous thermal insulation

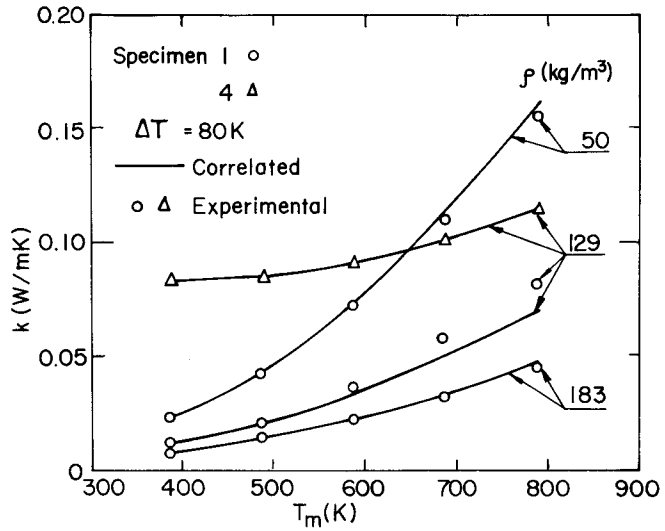

Fig. 4 Thermal conductivity vs. averaged material temperature

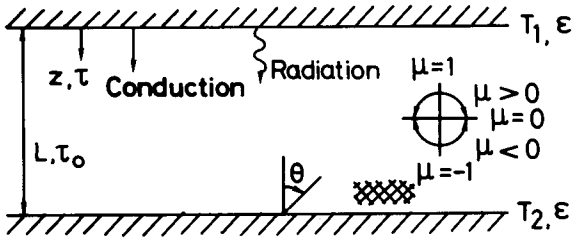

Fig. 5 Heat transfer model and coordinate system

and the coordinate system are shown. The following assumptions were adopted in the present analysis.

1. The insulation system is infinitely plane parallel.
2. The heat transfer in the thermal insulation between two heaters is governed by radiation and conduction.
3. The fiber matrix in the thermal specimen layer behaves apparently as a gray body on radiation, and the scattering of radiaion beam in the layer is isotropic.
4. The specimen does not change chemically in the experimental temperature range.

The energy equation is expressed as follows;

$$\frac{d}{dz}\left\{-k_c\left(\frac{dT}{dz}\right)+q_r(z)\right\}=0 \tag{2}$$

where k_c is the conduction thermal conductivity of the insulation layer. The boundary conditions are;

$$T(z=0)=T_1 \text{ and } T(z=L)=T_2 \tag{3}$$

The radiative heat flux $q_r(z)$ is expressed by the following equation;

$$q_r(z)=2\pi\int_0^{\infty}\int_{-1}^{+1} I_\lambda(z,\mu)\mu d\mu d\lambda \tag{4}$$

where μ is the direction cosine and λ is the spectral subscript. The spectral radiative intensity $I_\lambda\ (z,\mu)$ can be obtained by solving the following radiative transfer equation[6];

$$\mu\frac{dI_\lambda(\tau,\mu)}{d\tau}=-I_\lambda(\tau,\mu)+\frac{\tilde{\omega}}{2}\int_{-1}^{+1} I_\lambda(\tau,\mu)d\mu+(1-\tilde{\omega})\ I_{b\lambda}(\tau) \tag{5}$$

where $\tau=K_e\cdot z$, τ is the optical thickness, K_e is the extinction coefficient, $\tilde{\omega}$ is the scattering albedo, and $I_{b\lambda}$ is the blackbody emission source. The boundary surfaces are assumed to be diffuse. Then, the boundary conditions are as follows;

$$\begin{aligned} &I_\lambda(0,\mu)=\varepsilon I_{b\lambda}(T_1)+2(1-\varepsilon)\int_0^1 I_\lambda(0,\mu')\mu' d\mu' \qquad (\mu<0)\\ &I_\lambda(\tau_o,\mu)=\varepsilon I_{b\lambda}(T_2)+2(1-\varepsilon)\int_0^1 I_\lambda(\tau_o,-\mu')\mu' d\mu', \qquad (\mu>0) \end{aligned} \tag{6}$$

3. 3 Evaluation of conduction thermal conductivity

Before the calculation of the radiation heat flux q_r from the observed conductivity, which is composed of contributions of conduction and radiation by Eq. (2), it is necessary to evaluate the conduction thermal conductivity k_c of the specimen under vacuum. As far as the insulations at high temperature and vacuum conditions are concerned, the contribution of k_c to the thermal conductivity k would be not so large compared with the one of radiation, because the

radiation heat flux predominates over the conduction heat flux. Then, the next simple expression of k_c, which would be roughly evaluated, was adopted;

$$k_c(\rho, T_m) = C \cdot V_s \cdot k_s(T_m) \tag{7}$$

where k_s is the characteristic (or true) thermal conductivity of the fiber of the insulating material which depends on the material temperature, V_s is the volumetric fraction of the fiber which is a function of the bulk density of the insulating material, C is a constant. The value of C was determined in the following manner; Two apparent thermal conductivities of Specimen 1 were observed for $\rho = 50\ \mathrm{kg/m^3}$ and $183\ \mathrm{kg/m^3}$ at $T_m = 323\ \mathrm{K}$, $\Delta T = 40\ \mathrm{K}$ and $L = 0.03\ \mathrm{m}$. Assuming that the heat transfer was performed only by radiation, the extinction coefficient per unit bulk density, K_e/ρ, for $\rho = 50\ \mathrm{kg/m^3}$ was determined from the observed conductivity by solving numerically the set of the equations from Eq. (2) to Eq. (6). The set was solved again for $\rho = 183\ \mathrm{kg/m^3}$ using the observed conductivity and the above value of K_e/ρ so as to give the best fit value of k_c through Eq. (2). From this value of k_c, Eq. (7) gives $C = 0.0018$, which would be a minimum value for C, because the contribution of radiation for $\rho = 183\ \mathrm{kg/m^3}$ was probably overestimated. As a maximum value of C, $C = 0.005$ was adopted from the model proposed by Thornburgh et. al.[7]. Ignoring the contribution of radiation for the observed conductivity of $\rho = 183\ \mathrm{kg/m^3}$, almost the same value of C ($= 0.005$) was obtained. Finally, the averaged value $C = 0.0034$ between 0.0018 and 0.005 was adopted for Eq. (7) to all the specimens.

3. 4 Determination of extinction coefficient

There are two kinds of optical coefficients, that is, the extinction coefficient and the albedo, which govern the radiation heat transfer in the material. These two coefficients can be determined from the observed heat flux through solving the set of Eqs. (2) - (6). Among them, the albedo was hardly determined, because this coefficient does not have an appreciable effect on the heat flux in the range of large optical thickness such as in the present experiment where the optical thickness ranged larger than 20. In preliminary calculations, practically the same values of the extinction coefficients were obtained for albedo between 0.1 and 0.95. Then, it was assumed that $\bar{\omega} = 0.5$ for all calculations. As to the extinction coefficient, it is only assumed to be proportional to the bulk density ρ. The emissivity of the boundary surface was assumed to be $\varepsilon = 1$. The calculation procedure of K_e was as follows;

1. A value of K_e is assumed.
2. A temperature distribution in the material is assumed.

3. The radiation intensity I_λ is numerically calculated by Eqs. (5) and (6).
4. The radiation heat flux $q_r(z)$ is calculated from Eq. (4), by using the intensity obtained above.
5. The temperature distribution is calculated again from Eq. (2), by inserting the obtained q_r (z).
6. The above mentioned set of calculations is iterated until the temperature distribution converges.
7. The total heat flux is calculated from q_r (z) and the temperature distribution obtained.
8. The assumption of K_e is repeated until agreement is obtained between the calculated and the observed total heat flux so as to determine the value of K_e.
9. The assumption of K_e is repeated again until the least square of differences between the calculated and the observed heat fluxes for all of the bulk densities of a specimen is obtained, under the assumption that K_e is proportional to the bulk density. The calculated results of the procedure are drawn as the solid lines in Fig. 4.

4. Discussions

4. 1 Extinction coefficient

Figure 6 shows the relation of K_e/ρ and T_m by analyzing the experimental results for $\Delta T = 80$ K. As seen in the figure, K_e/ρ is not constant, but somewhat

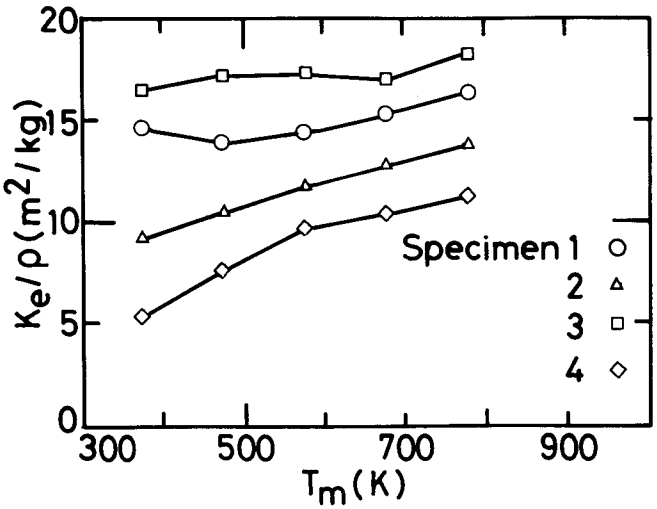

Fig. 6 Relation between K_e/ρ and T_m

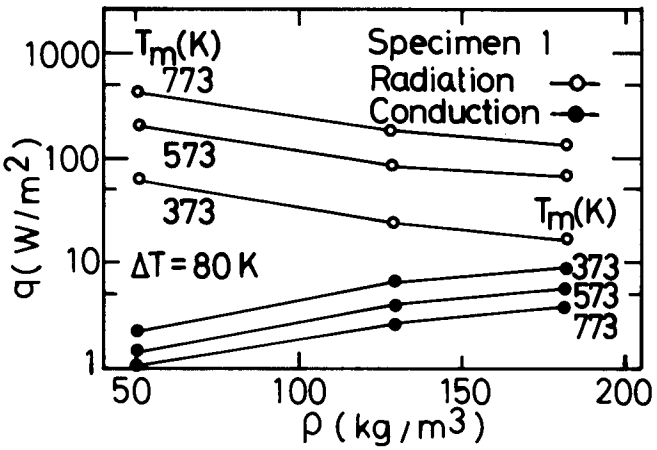

Fig. 7 Comparison of radiation and conduction heat flux

increases with the mean material temperature.

4. 2 Comparison of radiation and conduction heat flux

Figure 7 demonstrates an example of the comparison of the calculated radiation and conduction heat flux for Specimen 1 at $L = 0.03$ m. The contribution of radiation is far larger than that of conduction at a low bulk density. By increasing the bulk density, the contribution of radiation gradually decreases. Their difference becomes insignificant as the temperature decreases.

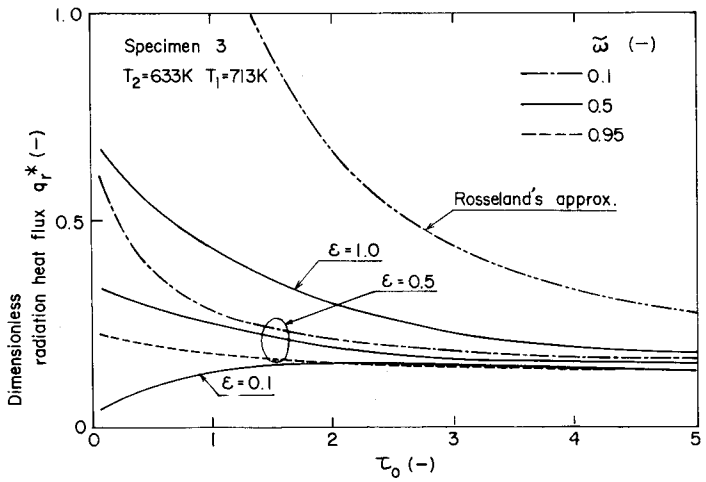

Fig. 8 Relation between dimensionless radiation heat flux and totoal optical thickness of insulation layer

4. 3 Relation between radiation heat flux and optical thickness

Figure 8 shows an example of the effect of the optical thickness on the radiation heat flux for Specimen 3. The heat flux is given as the dimensionless radiation heat flux. The value of q_r is significantly influenced by albedo and the emissivity of the hot and cold boundary surface, ε. The effect of albedo reaches further than the boundary emissivity. In any event, for this example, the effects of these three factors almost disappear at $\tau_0 = 5$. Thereafter those fluxes for different parameters gradually coincide and asymptote to the flux given by Rosseland's approximation;

$$q_r^* = (4/3)(1/\tau_0) \tag{8}$$

4. 4 Relation between thermal conductivity and thickness of fiber mat

Figure 9 shows an example of the calculated thermal conductivity of Specimen 1 using the observed extinction coefficient. Above $L = 5 \times 10^{-2}$ m, con-

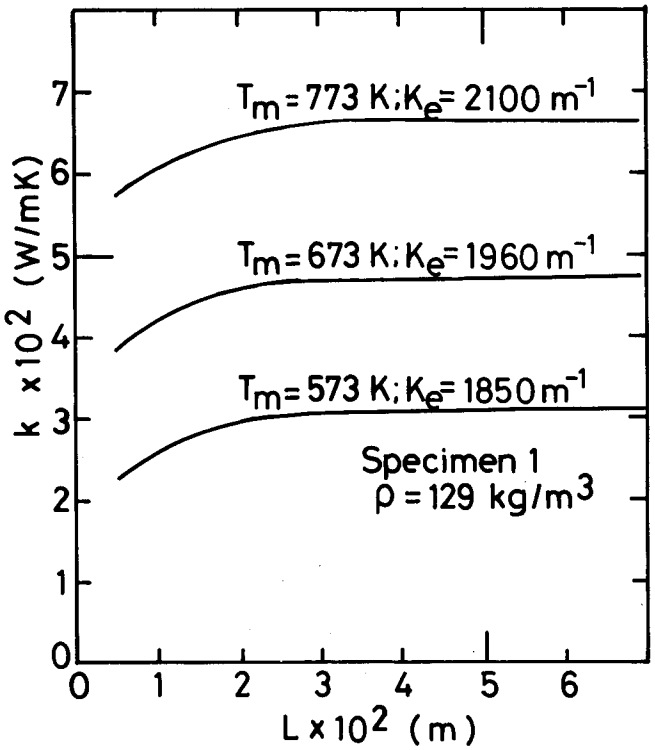

Fig. 9 Relation between calculated thermal conductivities and thickness of Specimen 1

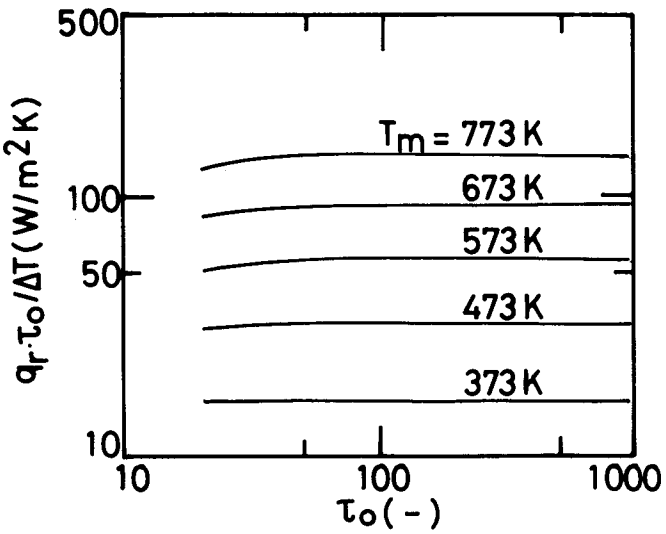

Fig. 10 Relation between $q_r\tau_o/\Delta T$ and τ_o

ductivities are almost constant. However, below that thickness, they gradually decrease as the thickness decreases.

4. 5 Calculation chart for radiation heat flux

Figure 10 shows the relation between $q_r \cdot \tau_o/\Delta T$ and τ_o. The former variable corresponds approximately to the product of the radiation thermal conductivity and the extinction coefficient. The curves are the numerical solutions for Eqs. (2) - (7), based on albedo $\tilde{\omega} = 0.5$. Because the influence of albedo is not significant in the range of albedo between 0.1 and 0.95, except for a very small optical thickness less than $\tau_o = 20$, the results in this figure are thought to be practically applicable for the approximate estimation of radiation heat flux of the fiber mat. The estimation procedure is as follows:

1. From the given thickness of the fiber mat and the extinction coefficient, the optical thickness, τ_o, is calculated.
2. From Fig. 10, the value of $q_r \cdot \tau_o/\Delta T$ is found.
3. By multiplying the above value by the temperature difference between the hot and the cold surface and dividing by the optical thickness, the radiation heat flux is estimated.

The above estimation procedure would be useful for the thermal insulation design, when the extinction coefficient is known.

5. Conclusions

1. The thermal conductivities of three kinds of commercial thermal insulation fiber mats and a graphite fiber mat under vacuum condition were measured at various bulk densities and temperatures.
2. The extinction coefficients of those four kinds of fiber mats were determined by solving the rigorous radiation energy transfer equations.
3. A calculation chart to estimate the radiation heat flux was given, based on the rigorous solutions of the radiation energy transfer equations.

Acknoledgments

The authors wish to thank Prof. M. OKAZAKI and Dr. H. IMAKOMA of the Department of Chemical Engineering for their advice, and valuable discussions to accomplish this research.

A part of this research was supported by the Grant of General Sekiyu Research and Development Encouragement and Assistance Foundation, Tokyo, JAPAN, and by the Grant in Aid for Scientific Research from the Ministry of Education, Science and Culture of JAPAN.

Nomenclature

A=surface area of main heater (measuring part)	[m^2]
C=constant as defined in Eq. (7)	[−]
d=fiber diameter	[μm]
I_λ=monochromatic intensity of radiation	[W/ ($m^2 \cdot \mu m$)]
K_e=extinction coefficient ($=K_a+K_s$)	[m^{-1}]
K_a=absorption coefficient	[m^{-1}]
K_s=scattering coefficient	[m^{-1}]
k=thermal conductivity of insulation layer	[W/ (m • K)]
k_s=characteristic (or true) conductivity of fiber	[W/ (m • K)]
L=thickness of specimen	[m]
q=heat flux	[W/m^2]
q_r^*=dimensionless radiation heat flux [$=q_r/\{\sigma(T_1^4-T_2^4)\}$]	[−]
T=temperature	[K]
T_1=surface temperature of main heater	[K]
T_2=surface temperature of heat sink	[K]

T_m=mean temperature of insulation layer [K]
ΔT=temperature difference ($=T_1-T_2$) [K]
W=heat input to main heater [W]
V_s=volumetric fraction of fiber in mat [m^3-fiber/m^3-bed]
z=coordinate [m]
ε=emissivity of boundary surface [−]
θ=polar angle [−]
μ=cos θ [−]
ρ=bulk density [kg/m^3]
ρ_o=true density of fiber [kg/m^3]
σ=Stefan-Boltzmann constant ($=5.67\times10^{-8}$) [$W/(m^2K^4)$]
τ=optical thickness ($=K_e \cdot L$) [−]
$\tilde{\omega}$=single scattering albedo ($=K_s/K_e$) [−]

subscript

b=blackbody
c=conduction
m=mean
r=radiation
λ=spectral

Reference

1) C. Langlais, and S. Klarsfeld; J. Thermal Insulation, **8**, 49 (1984)
2) K. Kamiuto, I. Kinoshita, Y. Miyoshi and S. Hasegawa; J. Nuclear Sci. and Tech., **19**. 460 (1982)
3) C. Bankvall; J. Testing and Evaluation, **1**, 235 (1973)
4) R. Caps, J. Fricke, and H. Reiss; High Temperature-High Pressure, **17**, 303 (1985)
5) Y. Touloukian, P. Liley, and S. Sanena; "Thermophysical Properties of Matter, Non-metallic Solid", Plenum Press, New York (1970)
6) S. Chandrasekhar; "Radiative Transfer", Dover Publications, New York (1960)
7) T. D. Thhornburgh and C. D. Peers; ASME Paper, 65-WA/HT-4 (1965)